

Published in final edited form as:

Neuron. 2011 November 17; 72(4): 587–601. doi:10.1016/j.neuron.2011.08.029.

Recruitment of endophilin to clathrin coated pit necks is required for efficient vesicle uncoating after fission

Ira Milosevic^{*,1}, Silvia Giovedi^{*,1,2}, Xuelin Lou^{1,#}, Andrea Raimondi^{1,§}, Chiara Collesi^{1,4,†}, Hongying Shen¹, Summer Paradise¹, Eileen O'Toole³, Shawn Ferguson¹, Ottavio Cremona⁴, and Pietro De Camilli^{1,*}

¹Department of Cell Biology, Howard Hughes Medical Institute, Program in Cellular Neuroscience, Neurodegeneration and Repair; Kavli Institute for Neuroscience, Yale University School of Medicine, New Haven, CT 06519, USA

²Department of Experimental Medicine, University of Genova, Italy

³Boulder Laboratory for 3D Electron Microscopy of Cells, Department of Molecular, Cellular and Developmental Biology, University of Colorado, Boulder, CO 80309, USA

⁴Università Vita–Salute San Raffaele and IFOM (Istituto FIRC di Oncologia Molecolare), Milano, Italy

Abstract

Endophilin is a membrane binding protein with curvature-generating/sensing properties that participates in clathrin-dependent endocytosis of synaptic vesicle membranes. Endophilin also binds the GTPase dynamin and the phosphoinositide phosphatase synaptojanin, and is thought to coordinate constriction of coated pits with membrane fission (via dynamin) and subsequent uncoating (via synaptojanin). We show that although synaptojanin is recruited by endophilin at bud necks before fission, the knockout of all three mouse endophilins results in the accumulation of clathrin-coated vesicles but not of clathrin-coated pits at synapses. The absence of endophilin impairs, but does not abolish synaptic transmission and results in perinatal lethality, while partial endophilin absence causes severe neurological defects, including epilepsy, and neurodegeneration. Our data supports a model in which endophilin recruitment to coated pit necks, due to its curvature-sensing properties, primes vesicle buds for subsequent uncoating after membrane fission, without being critically required for the fission reaction itself.

Synaptic transmission relies on the fusion of synaptic vesicles (SVs) with the presynaptic plasma membrane (exocytosis) to release neurotransmitters. After exocytosis, excess plasma membrane resulting from the addition of SV membrane is rapidly internalized by compensatory endocytosis and used to generate new SVs. Proper nervous system function relies critically on the efficiency of this membrane recycling traffic.

*Correspondence should be addressed: pietro.decamilli@yale.edu, 1-203-737-4461.

*These authors contributed equally

#Current address: Department of Neuroscience, University of Wisconsin, Madison, WI, USA

§Department of Neuroscience and Brain Technology, IIT, Genova, Italy

†Current address: ICGEB, Trieste, Italy

Publisher's Disclaimer: This is a PDF file of an unedited manuscript that has been accepted for publication. As a service to our customers we are providing this early version of the manuscript. The manuscript will undergo copyediting, typesetting, and review of the resulting proof before it is published in its final citable form. Please note that during the production process errors may be discovered which could affect the content, and all legal disclaimers that apply to the journal pertain.

Clathrin-mediated endocytosis is a major pathway for SV recycling (Dittman and Ryan, 2009; Heuser and Reese, 1973). In this process, nucleation and growth of the clathrin coat helps gather proteins to be internalized and generates/stabilizes the bilayer curvature required for the formation of the endocytic bud. PI(4,5)P₂, a phosphoinositide selectively enriched in the plasma membrane, plays a key role in the recruitment and assembly of the endocytic clathrin adaptors which, in turn, recruit and promote the assembly of clathrin (Di Paolo and De Camilli, 2006). After a deeply invaginated clathrin-coated pit (CCP) is generated, it undergoes fission with the help of the GTPase dynamin (Ferguson et al., 2007; Raimondi et al., 2011) and then rapidly loses its coat. The clathrin disassembly reaction is mediated by Hsc70 (an ATP-dependent chaperone) and auxilin (a J-domain containing cofactor for Hsc70)(Guan et al., 2010; Yim et al., 2010), while shedding of the adaptors requires degradation of PI(4,5)P₂, via the action of PI(4,5)P₂ phosphatases, primarily synaptojanin (Cremona et al., 1999; Hayashi et al., 2008). These reactions are assisted by a variety of accessory factors, which prominently include members of the BAR domain containing protein superfamily (Frost et al., 2009; Peter et al., 2004).

BAR domains undergo dimerization to generate membrane-associated modules, which most typically have a crescent shape with a basic, membrane-binding surface at their convex surface. These modules bind curved bilayers and function as curvature sensors and/or inducers (Antonny, 2006; Frost et al., 2009; Peter et al., 2004). An abundant endocytic BAR domain-containing protein is endophilin A (referred to henceforth as endophilin), which is conserved from yeast (Rvs167) to mammals, where it is encoded by three different genes [SH3GL2, SH3GL1 and SH3GL3 encoding endophilin 1, 2 and 3 respectively] (de Heuvel et al., 1997; Ringstad et al., 1997). The N-terminal BAR domain of endophilin is followed, after a short sequence, by a C-terminal SH3 domain whose major interactors in the nervous system are dynamin and synaptojanin. The three endophilins have different patterns of expression, but are all expressed in the brain, with endophilin 1 being the most abundant isoform (de Heuvel et al., 1997; Ringstad et al., 1997; Ringstad et al., 2001).

While endophilin has been extensively investigated, its precise function remains debated. Its molecular properties suggest a role in coordinating CCP neck constriction, via its BAR domain, with the recruitment of both dynamin (to mediate CCP fission from the plasma membrane) and synaptojanin (to help in uncoating), via its SH3 domain. Indeed, endophilin is recruited to CCPs shortly before fission (Perera et al., 2006) and independently of dynamin recruitment (Ferguson et al., 2009).

Microinjection experiments at the lamprey giant axon and genetic studies in *Drosophila* and *C. elegans* have explored endophilin functions at synapses. While initial experiments in the lamprey model had suggested both early and late actions of endophilin in clathrin-mediated budding (Ringstad et al., 1999), subsequent studies have indicated primarily late actions (Dickman et al., 2005; Gad et al., 2000; Schuske et al., 2003; Verstreken et al., 2002; Verstreken et al., 2003), consistent with the recruitment of endophilin at CCPs shortly before fission. An accumulation of clathrin coated vesicles (CCVs), reflecting a major role in uncoating, was the predominant consequence of the disruption of endophilin function in these studies, but a build-up of budding intermediates was also reported, consistent with a role of endophilin in fission (Gad et al., 2000; Schuske et al., 2003; Verstreken et al., 2002; Verstreken et al., 2003).

Evidence for a role of endophilin in fission also comes from its ability to co-assemble with dynamin in a tubular coat (Farsad et al., 2001; Sundborger et al., 2011) and by studies of endophilin (Rvs167) in budding yeast (Kaksonen et al., 2005). Further interest in a potential role of endophilin in fission was elicited by the proposal that synaptojanin-dependent PI(4,5)P₂ dephosphorylation is directly implicated in the fission reaction by generating a line

tension between the PI(4,5)P₂-rich plasma membrane and a PI(4,5)P₂-depleted deeply invaginated coated bud (Liu et al., 2009). Thus, endophilin could participate in fission via its interaction with both dynamin and synaptojanin. However, an essential action of endophilin and synaptojanin in fission contrasts with the prominent accumulation of CCVs but not of CCPs in synaptojanin 1 KO mice (Cremona et al., 1999; Hayashi et al., 2008). Finally, and surprisingly, a recent study suggested that the interactions of endophilin with dynamin and synaptojanin are not required for the role of endophilin in endocytic SV recycling (Bai et al., 2010).

To help dissect the role of endophilin at synapses, in particular in SV fission and uncoating, we have carried out an analysis of the effects produced by deletion of all three endophilin genes in mice. The most striking change observed at synapses without endophilin is an accumulation of CCVs without a change in the number of CCPs, supporting the idea that the major function of endophilin is to couple fission to uncoating in partnership with synaptojanin and Hsc70/auxilin. We also show that synaptojanin is recruited before fission and independently of dynamin, suggesting that depletion of PI(4,5)P₂ from the vesicle bud may precede fission. Collectively, these findings advance our understanding of the sequence of events underlying SV recycling, and more generally the process of clathrin-mediated endocytosis.

RESULTS

Synaptojanin 1 is recruited to endocytic clathrin coated pits upstream of dynamin

The accumulation of endophilin on the tubular stalks of the arrested endocytic CCPs in fibroblasts that lack dynamin [dynamin 1,2 double KO cells] proves that the recruitment of endophilin to the pits occurs before fission and independently of dynamin (Ferguson et al., 2009). However, it is unknown whether synaptojanin 1, in particular the synaptojanin 1 isoform that lacks clathrin and AP-2 binding sites (synaptojanin 1-145), is recruited upstream of dynamin as well. To address this question, fluorescently tagged synaptojanin 1-145, endophilin 2 and clathrin light chain (LC) were expressed in pair-wise combinations in dynamin double KO cells, which were then imaged by confocal microscopy.

In control cells, both endophilin and synaptojanin 1-145 had a primarily cytosolic distribution with only few transient puncta that coincided with a subpopulation of late stage CCPs (Perera et al., 2006)(Fig 1A and insets). By contrast, in cells without dynamin, numerous synaptojanin 1-145 bright spots were present (Fig 1B), that colocalized with the intense endophilin signal previously shown to represent the tubular stalks of arrested CCPs (Fig 1B and insets)(Ferguson et al., 2009). Accordingly, these spots appeared as short elongated elements adjacent to clathrin spots (Fig 1C–D). Interestingly, the EGFP-tagged BAR domain-only of endophilin (aa 1–247) was also recruited to the base of the arrested CCPs (Fig 1C), indicating that targeting of endophilin to endocytic CCPs does not require the SH3 domain. Most likely, the recruitment of the BAR domain to CCP stalks is due to its propensity to bind PI(4,5)P₂-rich, highly curved membranes (Antonny, 2006; Chang-Ileto et al., 2011; Cui et al., 2009; Ferguson et al., 2009; Frost et al., 2009; Madsen et al., 2010; Peter et al., 2004).

Synaptojanin 1-145 was no longer recruited to the arrested CCPs of dynamin KO cells following the siRNA dependent knock-down of endophilin 2, the major endophilin isoform in fibroblasts (Fig 1E–G). We conclude that synaptojanin 1-145 is recruited before fission and that endophilin plays a primary role in its recruitment (see model in Fig 1D). Overall, these findings strongly support a scenario in which the actions of endophilin and synaptojanin begin before fission. To gain new insight into the relation of endophilin to membrane fission and vesicle uncoating we generated mice that lack endophilin.

Absence of endophilins causes perinatal lethality

The endophilin 1 gene was inactivated by deleting exon 1 (Fig S1A). Surprisingly, endophilin 1 KO mice had a normal life span and no obvious phenotypic defects, suggesting a functional compensation by endophilin 2 and/or 3. Therefore we disrupted the two other genes. Endophilin 2 KO mice were obtained by deleting all exons except exon 1 (Fig S1A). For endophilin 3, a conditional allele was first generated by floxing exon 1 (Fig S1A), and KO mice were subsequently obtained by mating endophilin 3 conditional KO mice to β -actin-Cre mice. Both endophilin 2 and endophilin 3 single KO mice appeared normal and fertile.

The single KO mice were bred to each other to generate double and triple KO mice. While endophilin 1,3 and endophilin 2,3 double KO mice lived to adulthood (Fig S1B), endophilin 1,2 double KO mice (henceforth DKOs) appeared normal at birth, but approximately 30% of them died within 24 h (71/246 animals from 35 litters)(Fig 2A, 2C). The remaining mice survived up to 3 weeks, but had a compromised growth curve (Fig 2C–D) and major neurological defects, as revealed by poor motor coordination (Movie S1 and see below) and spontaneous epileptic seizures (Movie S2). Endophilin triple KO (TKO) mice were born according to Mendelian ratio (75/315 animals from 56 litters born to $E1^{-/-}E2^{+/-}E3^{-/-}$ parents), but were distinguishable from their littermates immediately after birth due to their slightly smaller size, breathing problems and lack of milk in their stomachs (Fig 2B, 2D). They died immediately or within a few hours after birth (Fig 2C). Mice with a single WT endophilin 2 allele ($E1^{-/-}E2^{+/-}E3^{-/-}$) lived to adulthood, but had severe epileptic seizures (Fig S1C, Movie S3).

Lack of expression of the respective endophilin isoform in each of the mutant genotypes was confirmed by western blot analysis of brain homogenates with isoform-specific antibodies and a pan-endophilin antibody (Fig 2E). These results were further validated by western blotting of material that had been affinity purified from newborn brain extracts by a high affinity ligand for all three endophilins: the proline-rich domain (PRD) of synaptojanin 1-145 (Fig 2E). Since we were interested in the basic functions of endophilin in nerve cells, we focused our subsequent studies on neurons of TKO mice, although we also carried out selected experiments on endophilin 1,2 DKOs.

No abnormalities were observed in the newborn TKO brain upon gross histological examination. Immunoblot studies of TKO brain homogenates did not show significant changes relative to wild-type (WT) in the levels of clathrin-coat proteins and other endocytic proteins (clathrin, α -adaptin, AP-180, dynamin, amphiphysin, SNX9, auxilin, Hsc70), with the exception of syndapin/pacsin and synaptojanin, whose levels were decreased (Fig 2F). Significant reductions were also observed for intrinsic (synaptobrevin 2, synaptophysin, synaptotagmin 1, vGLUT1 and vGAT) and peripheral (synapsin 1, Rab3a and GAD65) SV proteins (Fig 2F). However, the post-synaptic protein PSD95 did not show any change, arguing against a reduction in the number of synapses.

Synaptic transmission is impaired but not abolished in neurons lacking endophilin

The occurrence of some movement in endophilin TKO newborn mice prior to their death indicates that neurotransmission is not completely impaired. We therefore analyzed synaptic transmission in dissociated cortical neuronal cultures from these mice by whole-cell voltage-clamp recordings.

While TKO neurons in culture differentiated normally and appeared healthy, miniature excitatory postsynaptic currents (mEPSC) had strongly reduced frequency (over 2.5 times; Fig 3A), and a decreased amplitude (69.7% of control) that was not due to a smaller SV size (Fig S3A). Responses to a single stimulus revealed a reduction in EPSC peak amplitude in

TKO synapses relative to WT (Fig 3B). This change may reflect, at least in part, a reduction in SV number, as shown below in Fig 5. The property of cells without endophilin to maintain secretion in response to a sustained stimulus was also compromised. The synaptic depression produced by a 30 AP/10 Hz stimulus was enhanced in TKO neurons (Fig 3C), although no difference was observed when same number of stimuli was delivered at 1 Hz. To monitor a potential defect in recovery, neurons were next subjected to a strong stimulus (300 AP at 20 Hz). Not only synaptic depression was enhanced, but the recovery was also significantly delayed in TKOs (Fig 3D). Thus, the endophilins are not essential for synaptic transmission but are required for efficient and sustained evoked release consistent with studies in invertebrates (Dickman et al., 2005; Schuske et al., 2003; Verstreken et al., 2003).

Slower post-stimulus endocytic reinternalization of SV proteins in endophilin TKO synapses

To assess the potential occurrence of an endocytic delay, as expected if endophilin was involved in CCP fission, we performed dynamic assays of endocytosis using a synaptotHluorin-based strategy (Sankaranarayanan and Ryan, 2000). In TKO cells, the time constant of endocytic recovery following a 10 Hz stimulus for 30 s was approximately 2.5-fold slower in TKO (71.4 ± 15.8 s) than in WT (29.3 ± 5.2 s) (Fig 4A). Given sufficient time, however, the signal recovered and synapses could sustain multiple rounds of exo/endocytosis. Similar results were obtained with vGLUT1-pHluorin, a chimera of the vesicular glutamate transporter vGLUT1 with pHluorin (Voglmaier et al., 2006) (26.65 ± 6.7 s in WT and 82.2 ± 12 s in TKO) (Fig 4B). Thus, although the SH3 domains of endophilin 1 and 3 interact with vGLUT1 (Voglmaier et al., 2006), the defect in the compensatory endocytic recapture of this protein in endophilin TKO cells is not significantly more severe than the defect in the re-internalization of synaptobrevin.

In principle, the delayed post-stimulus recovery could be due to a delay in the acidification of the newly formed vesicles. However, a brief exposure to acid medium during the recovery (Sankaranarayanan and Ryan, 2000) demonstrated that the pHluorin responsible for the increased signal remained cell surface exposed, thus suggesting a bona fide endocytic delay (Fig 4F).

The slower kinetics of endocytosis in TKO neurons could be fully rescued by transfection with endophilin 1 (Fig 4C–E). In contrast, a mutant endophilin 1 construct that contains the BAR domain but that lacks the SH3 domain produced a limited rescue of the endocytic defect, and primarily during the late phase of the recovery (Fig 4C–E). Since the BAR domain of endophilin alone is recruited to the CCP neck, a possible interpretation of this partial rescue of endocytosis is a facilitatory/stabilizing effect of the overexpressed BAR domain on the vesicle neck.

Endophilin TKO synapses accumulate clathrin-coated vesicles but not clathrin-coated pits

To gain direct insight into whether the endocytic delay observed in TKO cultures was due to a block in fission, electron microscopy (EM) was performed. TKO synapses revealed a strikingly different phenotype relative to controls: reduced number of SVs and a strong accumulation of clathrin-coated vesicular profiles (Fig 5A–C). Surprisingly, no accumulation of CCPs was observed. In sections of some nerve terminals, nearly the entire pool of SVs had been replaced by clathrin-coated profiles (Fig 5B). Quantification of EM micrographs showed that the mean number of SVs per synapse was substantially lower (39.8%) in TKO than in controls, while the number of CCVs had increased more than 31 times (Fig 5F–I). Similar, but less severe changes, were observed at synapses of DKO neurons (Fig 5F–I).

The abundance and overall organization of clathrin-coated vesicular profiles in endophilin TKO synapses was reminiscent of that observed in synaptojanin 1 and dynamin 1 KO cultures (Cremona et al., 1999; Ferguson et al., 2007; Hayashi et al., 2008; Raimondi et al., 2011). In all three types of mutant synapses, coated vesicular profiles were sparsely packed and spatially segregated from the tightly packed SV clusters that remained anchored to the active zone, but were much smaller than in controls (Fig 5C–E). However, in dynamin KO synapses, many coated profiles had tubular necks clearly visible in a single section. In contrast, in both endophilin TKO and synaptojanin 1 KO synapses, such necks were not present and CCPs connected to the cell surface were extremely rare (Fig 5C–E), with no significant increase of CCPs in TKO relative to WT (Fig 5H). EM tomography confirmed the dramatic difference between control and endophilin KO synapses (Fig 5J–L), and demonstrated that, as in the case of synaptojanin 1 KO synapses, but in striking contrast with dynamin KO synapses (Ferguson et al., 2007; Hayashi et al., 2008; Raimondi et al., 2011), the overwhelming majority of coated profiles of endophilin TKO neurons were free CCVs (Fig 5L). Similar observations were made in tomograms of endophilin DKO synapses (Fig 5K).

Further evidence for lack of connection of coated vesicular profiles to the plasma membrane came from incubation of TKO cultures on ice with an endocytic tracer, horseradish peroxidase-conjugated cholera toxin (CT-HRP)(Fig S3B–C). Coated profiles of endophilin TKO synapses were not accessible to the tracer (Fig S3), in contrast to their accessibility in dynamin mutant synapses (Ferguson et al., 2007; Raimondi et al., 2011). However, when the incubation on ice was followed by a further incubation at 37°C for 1h, several CCVs of TKO synapses were positive for the HRP reaction product, indicating their recent formation and thus participation in membrane recycling. Labeled vesicles were primarily CCVs in the TKO, but SVs in WT, consistent with delayed uncoating in endophilin TKO neurons.

In conclusion, SV recycling is heavily backed-up at the CCV stage in TKO synapses. A plausible explanation for the discrepancy between the endocytic defect suggested by the pHluorin data and evidence for a post-fission (rather than fission) delay suggested by EM is that availability of endocytic proteins involved in steps leading to fission may be rate limiting due to their sequestration on CCVs. Such a scenario would be consistent with the reported accumulation of SV proteins at the plasma membrane when the function of endophilin is impaired (Bai et al., 2010; Schuske et al., 2003), an observation that we have also made in endophilin TKO synapses (Fig S2). Rate limiting availability of clathrin coat proteins is supported by fact that levels of such proteins were not increased in TKO neurons in spite of the dramatic increase in CCV number. Consistent with this explanation, an endocytic delay based on a pHluorin assay, in spite of a selective accumulation of CCVs but not of CCPs, was previously observed in studies of synaptojanin and auxilin KO synapses (Mani et al., 2007; Yim et al., 2010). It is also possible that the kinetic delay of endocytosis detected by the pHluorin assay may not be sufficiently robust to reflect an accumulation of CCPs. Regardless, EM data demonstrate that the key defect produced by the lack of endophilin is impaired uncoating.

Redistribution of endocytic proteins in nerve terminals in the absence of endophilin

Immunofluorescence analysis of the distribution of endocytic proteins in endophilin TKO cultures provided further support to the idea that a large fraction of such proteins is sequestered on assembled coats, and that the endophilin KO and synaptojanin KO phenotypes are similar. No difference was observed in the immunoreactivity pattern for the active zone marker Bassoon, indicating no overall difference in the formation, organization or number of synapses (Fig 6A). However, as reported for dynamin 1 KO and synaptojanin 1 KO neuronal cultures (Ferguson et al., 2007; Hayashi et al., 2008; Raimondi et al., 2011), the strong accumulation of clathrin-coated structures in nerve terminals (Fig 5) was reflected

by a stronger (relative to control) punctate synaptic immunoreactivity for endocytic clathrin coat components, namely clathrin itself (clathrin LC), α -adaptin (a subunit of AP-2) and AP180 (Fig 6A and B). Surprisingly, the two synaptic dynamins, dynamin 1 and 3 which are endophilin interactors, were also strongly clustered in both endophilin TKO and synaptojanin 1 KO synapses (Fig 6A–B). In contrast, the localization of synaptojanin 1 in endophilin TKO neurons was more diffuse than in the control (Fig 6A–B). These findings support the idea that endophilin is more important for the recruitment of synaptojanin than of dynamin to endocytic sites. Amphiphysin 1 and 2, which were also more clustered at endophilin TKO synapses, may participate in this recruitment (Fig 6A–B).

Rescue experiments to assess the specificity of endocytic protein clustering were performed by transfection of EGFP-clathrin LC (to selectively visualize clathrin in transfected cells) with or without Cherry-tagged endophilin constructs. Robust clustering of the clathrin signal was detected in cultures transfected with EGFP-clathrin LC alone (Fig 6C and S4). In contrast, the distribution of clathrin in cultures co-transfected with full length endophilin (see E1FL in Fig 6C) was diffuse and similar to the fluorescence observed in WT cultures (Fig 6C–D and S4). Importantly, when EGFP-clathrin LC was co-expressed with the endophilin BAR domain construct, no rescue was observed (Fig 6C–D and S4), demonstrating the importance of the SH3 domain for the rescue.

Additionally, the diffuse localization of synaptojanin 1 in endophilin TKO neurons (Fig 6A–B) could not be rescued by overexpression of the endophilin BAR construct (Fig S5). These data are in agreement with our observations in fibroblasts (Fig 1E–G) and indicate that the synaptojanin localization is dependent on interactions with endophilin's SH3 domain.

Auxilin was clustered both at endophilin TKO and synaptojanin 1 KO synapses. Thus, lack of clathrin uncoating does not result from impaired auxilin recruitment, but auxilin clearly does not achieve its function when recruited under these conditions. In contrast, auxilin did not cluster in dynamin 1 KO synapses (Fig 6A–B), where the overwhelming majority of clathrin-coated structures are pits, consistent with the previous report that auxilin is recruited to the sites of clathrin-mediated endocytosis only after membrane fission (Massol et al., 2006).

Finally, the clustering of endocytic proteins in both endophilin TKOs and synaptojanin 1 KO neurons was dependent on synaptic activity (Fig 6A), as in the case of dynamin KO synapses (Ferguson et al., 2007; Raimondi et al., 2011). Overnight treatment with TTX to silence activity drastically decreased clustering (Fig 6A), a change likely due a reduction of exo-endocytosis and progression of accumulated coated structures to SVs.

Increased yield of clathrin coated vesicles upon subcellular fractionation

A fraction enriched in CCVs was obtained from WT and endophilin TKO cultures (DIV21) (Girard et al., 2005)(Fig 6E). As expected from the defect in CCV uncoating revealed by EM, the recovery of clathrin and the AP-2 α -subunit in such fraction relative to the starting homogenate was higher in TKO samples (Fig 6E, right panel). In contrast, the recovery of γ -adaptin, a subunit of the Golgi localized clathrin adaptor complex AP-1, was the same as in controls, confirming a selective increase of endocytic CCVs. Importantly, the recovery of auxilin and Hsc70 was also increased in the TKO samples confirming that defective uncoating is not due to deficient recruitment of these proteins to coats. The even higher increased recovery of dynamin and amphiphysin was unexpected because these two proteins are typically not enriched in CCV fractions (Fig 6E)(Blondeau et al., 2004). Such an increase is consistent with the increased clustering of dynamin and amphiphysin in neuronal cultures seen by immunofluorescence and may reflect an overall defect in the shedding of endocytic proteins due impaired synaptojanin recruitment and PI(4,5)P₂ dephosphorylation.

Collectively, these results emphasize the importance of endophilin for clathrin coat shedding in nerve terminals.

Neurodegeneration in endophilin 1,2 DKO mice

As discussed above (Fig 5), defects similar to those observed at TKO synapses were also observed in endophilin 1,2 DKO neuron cultures, although they were less severe. The survival up to 3 weeks of a subset of DKO mice (Fig 2) gave us the opportunity to explore the impact of these defects on neurons *in situ* at a postnatal stage when synaptogenesis is more advanced. As in neuronal cultures, the obvious difference from controls was the abundance of CCVs and the smaller size of the SV cluster (Fig 5M–N). At later times, signs of neurodegeneration appeared. These were investigated in greater detail in the cerebellum.

Hematoxylin and eosin (H&E) staining of the cerebellar cortex at P18 revealed numerous vacuolar spaces (reminiscent of spongiform neurodegeneration) randomly distributed within the granule cell layer (Fig 7A). EM analysis showed that these spaces contained membranes and cell debris (Fig 7B). Nearby mossy fiber terminals displayed the typical reduction in the number of SVs and an increase in CCV abundance (Fig 7C). Immunofluorescence staining for various neuronal markers demonstrated a striking change in the architecture of climbing fibers, as shown by double labeling with anti-vGLUT2 antibodies (markers of these fibers) and anti-IP₃ receptor antibodies (markers of Purkinje cells)(Fig 7D). Climbing fibers of DKO animals were thicker and shorter than in WT and only surrounded the proximal portion of the Purkinje cells' major dendrites. Even in this case, EM showed a reduction of SV number and an increase in CCVs (Fig 7E). Overall, these observations demonstrate that the absence of endophilin 1 and 2 in the intact brain results in neurodegeneration.

DISCUSSION

This study, which represents the first comprehensive genetic analysis of the mammalian endophilins, provides new insights into the sequence of events underlying the transition from a CCP to an uncoated endocytic vesicle at neuronal synapses. Our results demonstrate that a key function of the endophilin family at mammalian synapses is to facilitate clathrin uncoating, thus strongly supporting the hypothesis that a major role of endophilin is to recruit the PI(4,5)P₂ phosphatase synaptojanin to endocytic sites. These results emphasize the scaffold function of endophilin, which binds the membrane via its BAR domain and interacts with dynamin and synaptojanin via its SH3 domain. They demonstrate the much greater contribution of endophilin to vesicle uncoating than to membrane fission, suggesting that their likely function in fission is greatly overlapping with that of other BAR proteins that also bind to CCP necks. We further show that endophilin 1, 2 and 3 have at least partially redundant roles, and that even in the absence of all three endophilins neurotransmission and SV recycling is impaired but not abolished.

The perinatal lethality of TKO mice, and the severe neurological defects and short life spans of DKO mice, indicate that the collective actions of the endophilins become essential only after birth, most likely because their absence impacts the proper network activity of the nervous system. Partially impaired endophilin function during postnatal life, as it occurs in the endophilin DKO, results in early neurodegeneration. Interestingly, endophilin was recently reported to bind with high affinity to Parkin, one of the Parkinson's disease genes (Trempe et al., 2009), and also to Huntingtin and ataxin-2, two additional proteins implicated in neurodegenerative diseases (Ralser et al., 2005).

Endophilin, like synaptojanin, is primarily needed for uncoating during SV endocytosis

Endophilin is recruited to CCPs prior to membrane fission (Ferguson et al., 2009; Perera et al., 2006). Yet, the major ultrastructural defect produced by the impairment of endophilin is a back-up of SV recycling traffic at the stage of CCVs, not an accumulation of CCPs, as it would be predicted by a delay or block in the fission reaction. Thus, the phenotype of endophilin TKO nerve terminals is very similar to that of synaptojanin 1 KOs (Cremona et al., 1999; Hayashi et al., 2008), and both phenotypes are strikingly different from that of dynamin 1 KO synapses, which are characterized by an accumulation of CCPs instead of CCVs (Ferguson et al., 2007; Hayashi et al., 2008; Raimondi et al., 2011). These findings stress the importance of the partnership of endophilin with synaptojanin that had also been reported in invertebrates. More specifically, similar phenotypes had been detected in flies and worms harboring endophilin or synaptojanin mutations (Dickman et al., 2005; Schuske et al., 2003; Verstreken et al., 2003). Additionally, injection of a peptide that block the SH3 dependent interaction of endophilin in the lamprey giant axon had demonstrated a major defect in uncoating, as expected if the recruitment of synaptojanin was impaired (Gad et al., 2000).

While the studies mentioned above had also reported an accumulation of CCPs following perturbation of endophilin function (Gad et al., 2000; Schuske et al., 2003; Verstreken et al., 2003), we did not detect such increase at endophilin TKO mouse synapses. Our findings are consistent with the 10-fold greater affinity of the SH3 domain of endophilin for synaptojanin than for dynamin (Trempe et al., 2009). They are also in agreement with the observation that in a cell-free study involving brain cytosol and liposomes, the occlusion of endophilin's SH3 domain with an inhibitory peptide nearly completely blocked the recruitment of synaptojanin to liposomes, but only had a modest effect on dynamin recruitment (Gad et al., 2000).

The concept that a major function of endophilin is to recruit synaptojanin contrasts with the conclusion of a recent study in *C. elegans* demonstrating that an exogenous endophilin construct lacking the SH3 domain is sufficient to rescue the viability and endocytic defect of endophilin mutant worms (Bai et al., 2010). In principle, the functional link between endophilin and synaptojanin may not be mediated exclusively by their SH3-dependent interaction. However, the evolutionary conservation of the SH3-dependent interaction from lower organisms to mammals suggests its critical importance. In fact, in our present study a BAR domain construct was targeted to the CCP necks, but did not rescue the clathrin accumulation phenotype, and it only produced a partial rescue of compensatory endocytosis in the pHluorin-based assay. This partial rescue could be the result of heterodimerization with other BAR domain proteins or of a facilitating/stabilizing effect on the vesicle neck (the pre-fission intermediate). It is also possible that the BAR domain may promote some form of clathrin-independent endocytosis, considering that rescue experiments with exogenous proteins are likely to result in at least some degree of overexpression (Bai et al., 2010).

While our data and previous studies emphasize the major similarity of the defects produced by the absence of either endophilin or synaptojanin 1, one notable difference was observed. In contrast to what we have found here at endophilin TKO synapses, the amplitude of mEPSCs was increased relative to control at synaptojanin 1 KO synapses. Interestingly, a similar discrepancy was observed in *Drosophila*, where other properties of endophilin and synaptojanin mutant synapses were similar (Dickman et al., 2005). Determining whether this discrepancy is due to a different impact of the lack of endophilin and of synaptojanin on postsynaptic functions is an interesting question for future investigations.

Endophilin and membrane curvature

Endophilin's bilayer deforming properties had suggested that it helps bend the membrane at CCPs, perhaps starting early in the process and then shaping their neck (Farsad et al., 2001; Gallop et al., 2006; Ringstad et al., 1999). However, imaging data have demonstrated that endophilin is recruited only shortly before fission, when most of the curvature of the bud and of its neck is already acquired (Ferguson et al., 2009; Perera et al., 2006).

Proteins suited to bind curved bilayers may function as curvature inducers or sensors depending on several parameters, including their concentration, bilayer chemistry and a variety of regulatory mechanisms (Antonny, 2006). Both curvature sensing and generating properties of endophilin were directly demonstrated (Chang-Ileto et al., 2011; Cui et al., 2009; Farsad et al., 2001; Madsen et al., 2010). Curvature sensing may predominate in the initial recruitment of endophilin at CCP necks, although additional polymerization may facilitate curvature stabilization and neck elongation. Our observation that the endophilin BAR construct is targeted to the CCPs supports this possibility. Consistent with this scenario, absence of the endophilin homologue Rvs167 in yeast leads to endocytic invaginations that bounce back and forth and often do not proceed to fission, suggesting a role of Rvs167 in stabilizing a pre-formed invagination (Kaksonen et al., 2005). An action of endophilin before fission, even if one of its main effects becomes manifested only after fission, also agrees with the finding that a plasma membrane tethered endophilin-chimeric construct rescued the absence of endophilin in worms (Bai et al., 2010).

The clathrin uncoating reaction

The role of Hsc70 and its co-chaperone auxilin in the disassembly of the clathrin lattice is well established. However, Hsc70/auxilin recruitment cannot account for the shedding of the adaptors from the membrane, a process that requires PI(4,5)P₂ dephosphorylation (Cremona et al., 1999; Hayashi et al., 2008). It was proposed that the synaptojanin's phosphatase activity triggers both adaptor shedding and auxilin recruitment (Guan et al., 2010), thus providing an efficient coordination of the two events to promote uncoating. Since auxilin recruitment follows dynamin-dependent fission (Massol et al., 2006), this scenario implies a selective action of synaptojanin after fission. However, recruitment of endophilin and synaptojanin upstream of dynamin (this study) and presence of auxilin, but not synaptojanin and endophilin on CCVs (Blondeau et al., 2004), favors a dissociation of the two events. Furthermore, we have found that while auxilin is not clustered at dynamin KO synapses, confirming its post-fission recruitment, it is clustered in endophilin TKO and synaptojanin 1 KO synapses. Thus, the function of synaptojanin is dispensable for auxilin recruitment, although it remains possible that it may be needed for its function. Perhaps, when auxilin is recruited under these conditions, such as by interactions with clathrin and AP-2, its catalytic domain is not engaged at the membrane and thus is not active. Furthermore, even if auxilin and Hsc70 were able to disassemble the clathrin lattice on CCVs of synaptojanin KO and endophilin TKO synapses, persistence of PI(4,5)P₂, and thus of the adaptors, on the vesicles would result in continuous clathrin reassembly. It is the shedding of the adaptors that makes clathrin disassembly an irreversible process. The presence of these two proteins at the vesicle neck implies that they may prime the vesicle for uncoating before fission occurs.

A putative model of clathrin-coated vesicle fission and uncoating at synapses

This study, along with our results on dynamin (Ferguson et al., 2007; Raimondi et al., 2011) and synaptojanin (Cremona et al., 1999; Hayashi et al., 2008), suggests the following sequence of events (Fig 8). Assembly and maturation of endocytic CCPs is independent of endophilin, which is recruited only to the highly curved bud neck, due to its curvature-sensing properties. Such recruitment may be amplified in a feed-forward mechanism by the property of endophilin to stabilize curvature and to assemble in a polymeric tubular coat via

its BAR domain. However, the dynamin-endophilin interaction is not required for the recruitment of either endophilin (Ferguson et al., 2009) or dynamin [(Gad et al., 2000) and this study]. Since endophilin can inhibit dynamin's GTP activity (Farsad et al., 2001), it may be part of a check-point mechanism to ensure that dynamin acts only at the optimal time.

In contrast, the recruitment of synaptojanin by endophilin at the vesicle stalk is important for the fate of the vesicles after fission. PI(4,5)P₂ dephosphorylation by synaptojanin may result in a PI(4,5)P₂-depleted compartment only above the vesicle neck due to the presence around the neck of a collar (comprising endophilin, other BAR proteins and possibly dynamin) that prevents PI(4,5)P₂ diffusion from the surrounding PI(4,5)P₂-rich plasma membrane. Conversely, depletion of PI(4,5)P₂ under the clathrin lattice covering the bud is not sufficient to promote uncoating prior to fission since the recruitment of auxilin/Hsc70 to disassemble the clathrin lattice requires fission, and the assembled cage cannot be released from the membrane because of its narrow neck. In turn, persistence of the clathrin lattice on the deeply invaginated bud, in spite of the loss of PI(4,5)P₂, prevents adaptor shedding due to the multiple interaction of the adaptors with both cargo and clathrin (Traub, 2009). Our model is consistent with the suggestion that PI(4,5)P₂ dephosphorylation also plays a role in fission because the generation of a boundary between a PI(4,5)P₂-rich and a PI(4,5)P₂-poor environment could generate a line tension that assists the action of dynamin in this process (Chang-Ileto et al., 2011; Liu et al., 2009). However, since SV endocytosis proceeds beyond fission even when the synaptojanin function is defective, the role of the line tension in fission, while very attractive, requires further experimental evidence. Likewise, other functions of endophilin, in particular non-endocytic functions like regulation of SV release probability (Weston et al., 2011), need to be investigated. It will also be interesting to determine whether the endophilin-synaptojanin partnership is as important in non-neuronal cells as it is at synapses. The endophilin KO mice that we have generated represent powerful tools for these studies.

EXPERIMENTAL PROCEDURES

Reagents and gene targeting strategies

Unless otherwise stated, all chemical were purchased from Sigma. Supplemental Information lists the antibodies used (Table S1) and describes gene targeting (Fig S1A) and cloning strategies.

Cell culture

Conditional dynamin 1,2 double KO mouse fibroblasts also expressing Cre-ER were treated with tamoxifen to induce recombination of the floxed dynamin 1 and 2 genes (dynamin KO cells)(Ferguson et al., 2009). RNAi-based KD of endophilin 2 in these cells was performed as in (Ferguson et al., 2009). EGFP-synaptojanin 1–145 (Perera et al., 2006), endophilin 2-Ruby and mRFP-clathrin LCa were expressed in these cells.

Primary cortical cultures were prepared as previously described from P0 brains (Ferguson et al., 2007). All constructs used in neurons were expressed, following AMAXA (Lonza, Basel, Switzerland) based transfection, under the control of the chicken- β -actin promoter to allow for long-term and even expression.

Biochemical procedures

For GST pull-downs, Triton X-100 extracts from WT and endophilin mutant P0 brains (~3 mg) were affinity-purified onto a GST fusion of synaptojanin 1's PRD domain (aa 1042–1310, 300 μ g). CCVs enriched fractions were prepared from 21 DIV neuronal cultures (see above) grown on poly-L-lysine coated dishes (~4 \times 10⁶/dish). 9–10 dishes for each genotype

were homogenized in 0.1M 2-(N-morpholino)ethanesulfonic acid, 1 mM EGTA, 0.5mM MgCl₂, protease inhibitors (Roche), pH 6.5. The lysate was then processed as in Girard et al. (2005). SDS-PGE and western blotting were carried out by standard procedure.

Fluorescence imaging

Immunofluorescence of frozen brain sections and cultured neurons (DIV 14–24) was carried as described (Ferguson et al., 2007; Ringstad et al., 2001). Fluorescent puncta were quantified as in (Hayashi et al., 2008). Data are presented as number of puncta per 100 μm^2 and are normalized to controls. At least 10 images from 3–6 experiments were analyzed for each genotype, and the t-test was used for the statistics. Live mouse fibroblasts were imaged using a Perkin Elmer Ultraview spinning-disk confocal microscope with 100 \times CFI PlanApo VC objective.

Electrophysiology

Cortical neurons were plated at a density of 50000–75000/cm² and examined at 20–22°C at DIV 10–14. Whole-cell patch clamp recordings were obtained using a double EPC-10 amplifier (HEKA Elektronik, Germany) and an Olympus BX51 microscope. Series resistance (R_s) was 3–5 M Ω and was compensated by 50–70% during recording. The pipette solution contained (in mM) 137 K-Gluconate, 10 NaCl, 10 HEPES, 5 Na₂-phosphocreatine, 0.2 EGTA, 4 Mg²⁺ATP, and 0.3 Na⁺GTP, pH 7.3. The extracellular solution contained (in mM): 122 NaCl, 2.5 KCl, 2 CaCl₂, 1 MgCl₂, 10 glucose, 20 HEPES, 20 μM bicuculin and 2 μM strychnine, pH 7.3. 1 μM TTX and 50 μM DAP5 were included in the above solution for mEPSC recordings. EPSCs were elicited by an extracellular stimulation electrode set at ~200 μm away from the recorded soma, the output of stimulation was controlled by an isolated pulse stimulator (Model 2100, AM Systems) and synchronized by Pulse software (HEKA). The holding potential was –70 mV for all the experiments without correction of liquid-junction potential. Data were analyzed with Igor Pro 5.04.

Optical imaging of vesicle dynamics

Imaging of neurons expressing synaptopHluorin or vGLUT1-pHluorin (Voglmaier et al., 2006) under the chicken- β -actin promoter was performed 13–20 days after plating essentially as described (Mani et al., 2007; Sankaranarayanan and Ryan, 2000). Neurons were subjected to electrical field stimulation at 10 Hz using a Chamliide stimulation chamber (LCI, Seoul, Korea) and imaged at RT in Tyrode solution containing (in mM) 119 NaCl, 2.5 KCl, 2 CaCl₂, 2 MgCl₂, 25 HEPES (pH 7.4), 30 glucose, 10 μM CNQX and 50 μM APV using a Nikon Eclipse Ti-E microscope with a 60 \times Apo (1.49 NA) objective and a EMCCD iXon 897 (Andor Technologies) camera. The average fluorescence of at least 48 fluorescent synaptic boutons was monitored over time and used to generate traces of the fluorescence signal by a custom written macro using Igor Pro 5.04. Data were normalized to the pre-stimulation fluorescence and fluorescence in ammonium chloride, and re-normalized to the maximum fluorescence after stimulation. Post-stimulation time constants were determined by fitting the post-stimulation fluorescent decay as described in (Sankaranarayanan and Ryan, 2000). For rescue experiments, rat endophilin 1 or endophilin 1 BAR (1–290) fused to mRFP (see Supplemental Information) were co-transfected with the pHluorins at the time of plating.

Electron microscopy and tomography

EM and EM tomography were carried out as described (Hayashi et al., 2008)(see also Supplemental Information). Quantitative analysis of SVs and clathrin coated structures was performed under blind experimental conditions using ITEM (Soft Imaging System,

Skillman, NJ). Data from 6 experiments were quantified and the t-test was used for the statistical analysis.

Supplementary Material

Refer to Web version on PubMed Central for supplementary material.

Acknowledgments

We thank L. Li, L. Lucast and F. Wilson for superb technical assistance, M. Messa for help with CCV purification, J. Baskin for discussion, G. Bertoni & R. Brescia (IIT, Genova, Italy) for help with tomography. We are grateful to L. Johnson and C. Zeiss (Yale Mice Research Pathology Facility) for histological analysis and to T. Nottoli (Yale Cancer Center Animal Genomics Shared Resource) for gene targeting. This work was supported in part by grants from the G. Harold and Leila Y. Mathers Charitable Foundation, the NIH (DK45735, DA018343 and NS36251), the W.M. Keck Foundation and a NARSAD Distinguished Investigator Award to PDC, grants from PRIN2008 to OC and SG, grants from Cariplo, Telethon and AIRC to OC, a pilot grant from the Yale DERC to XL, grant RR-000592 from the National Center for Research Resources of the NIH to A. Hoenger, and EMBO and Epilepsy Foundation fellowships to IM.

REFERENCES

- Antonny B. Membrane deformation by protein coats. *Curr Opin Cell Biol.* 2006; 18:386–394. [PubMed: 16782321]
- Bai J, Hu Z, Dittman JS, Pym EC, Kaplan JM. Endophilin functions as a membrane-bending molecule and is delivered to endocytic zones by exocytosis. *Cell.* 2010; 143:430–441. [PubMed: 21029864]
- Blondeau F, Ritter B, Allaire PD, Wasiak S, Girard M, Hussain NK, Angers A, Legendre-Guillemain V, Roy L, Boismenu D, et al. Tandem MS analysis of brain clathrin-coated vesicles reveals their critical involvement in synaptic vesicle recycling. *Proc Natl Acad Sci U S A.* 2004; 101:3833–3838. [PubMed: 15007177]
- Chang-Ileto B, Frere SG, Chan RB, Voronov SV, Roux A, Di Paolo G. Synaptojanin 1-mediated PI(4,5)P2 hydrolysis is modulated by membrane curvature and facilitates membrane fission. *Dev Cell.* 2011; 20:206–218. [PubMed: 21316588]
- Cremona O, Di Paolo G, Wenk MR, Luthi A, Kim WT, Takei K, Daniell L, Nemoto Y, Shears SB, Flavell RA, et al. Essential role of phosphoinositide metabolism in synaptic vesicle recycling. *Cell.* 1999; 99:179–188. [PubMed: 10535736]
- Cui H, Ayton GS, Voth GA. Membrane binding by the endophilin N-BAR domain. *Biophys J.* 2009; 97:2746–2753. [PubMed: 19917228]
- de Heuvel E, Bell AW, Ramjaun AR, Wong K, Sossin WS, McPherson PS. Identification of the major synaptojanin-binding proteins in brain. *J Biol Chem.* 1997; 272:8710–8716. [PubMed: 9079704]
- Di Paolo G, De Camilli P. Phosphoinositides in cell regulation and membrane dynamics. *Nature.* 2006; 443:651–657. [PubMed: 17035995]
- Dickman DK, Horne JA, Meinertzhagen IA, Schwarz TL. A slowed classical pathway rather than kiss-and-run mediates endocytosis at synapses lacking synaptojanin and endophilin. *Cell.* 2005; 123:521–533. [PubMed: 16269341]
- Dittman J, Ryan TA. Molecular circuitry of endocytosis at nerve terminals. *Annu Rev Cell Dev Biol.* 2009; 25:133–160. [PubMed: 19575674]
- Farsad K, Ringstad N, Takei K, Floyd SR, Rose K, De Camilli P. Generation of high curvature membranes mediated by direct endophilin bilayer interactions. *J Cell Biol.* 2001; 155:193–200. [PubMed: 11604418]
- Ferguson SM, Brasnjo G, Hayashi M, Wolfel M, Collesi C, Giovedi S, Raimondi A, Gong LW, Ariel P, Paradise S, et al. A selective activity-dependent requirement for dynamin 1 in synaptic vesicle endocytosis. *Science.* 2007; 316:570–574. [PubMed: 17463283]
- Ferguson SM, Raimondi A, Paradise S, Shen H, Mesaki K, Ferguson A, Destaing O, Ko G, Takasaki J, Cremona O, et al. Coordinated actions of actin and BAR proteins upstream of dynamin at endocytic clathrin-coated pits. *Dev Cell.* 2009; 17:811–822. [PubMed: 20059951]

- Frost A, Unger VM, De Camilli P. The BAR domain superfamily: membrane-molding macromolecules. *Cell*. 2009; 137:191–196. [PubMed: 19379681]
- Gad H, Ringstad N, Low P, Kjaerulf O, Gustafsson J, Wenk M, Di Paolo G, Nemoto Y, Crun J, Ellisman MH, et al. Fission and uncoating of synaptic clathrin-coated vesicles are perturbed by disruption of interactions with the SH3 domain of endophilin. *Neuron*. 2000; 27:301–312. [PubMed: 10985350]
- Gallop JL, Jao CC, Kent HM, Butler PJ, Evans PR, Langen R, McMahon HT. Mechanism of endophilin N-BAR domain-mediated membrane curvature. *EMBO J*. 2006; 25:2898–2910. [PubMed: 16763559]
- Girard M, Allaire PD, Blondeau F, McPherson PS. Isolation of clathrin-coated vesicles by differential and density gradient centrifugation. *Curr Protoc Cell Biol*. 2005; Chapter 3(Unit 3):13. [PubMed: 18228473]
- Guan R, Han D, Harrison SC, Kirchhausen T. Structure of the PTEN-like region of auxilin, a detector of clathrin-coated vesicle budding. *Structure*. 2010; 18:1191–1198. [PubMed: 20826345]
- Hayashi M, Raimondi A, O'Toole E, Paradise S, Collesi C, Cremona O, Ferguson SM, De Camilli P. Cell- and stimulus-dependent heterogeneity of synaptic vesicle endocytic recycling mechanisms revealed by studies of dynamin 1-null neurons. *Proc Natl Acad Sci U S A*. 2008; 105:2175–2180. [PubMed: 18250322]
- Heuser JE, Reese TS. Evidence for recycling of synaptic vesicle membrane during transmitter release at the frog neuromuscular junction. *J Cell Biol*. 1973; 57:315–344. [PubMed: 4348786]
- Kaksonen M, Toret CP, Drubin DG. A modular design for the clathrin- and actin-mediated endocytosis machinery. *Cell*. 2005; 123:305–320. [PubMed: 16239147]
- Liu J, Sun Y, Drubin DG, Oster GF. The mechanochemistry of endocytosis. *PLoS Biol*. 2009; 7:e1000204. [PubMed: 19787029]
- Madsen KL, Bhatia VK, Gether U, Stamou D. BAR domains, amphipathic helices and membrane-anchored proteins use the same mechanism to sense membrane curvature. *FEBS Lett*. 2010; 584:1848–1855. [PubMed: 20122931]
- Mani M, Lee SY, Lucast L, Cremona O, Di Paolo G, De Camilli P, Ryan TA. The dual phosphatase activity of synaptojanin I is required for both efficient synaptic vesicle endocytosis and reavailability at nerve terminals. *Neuron*. 2007; 56:1004–1018. [PubMed: 18093523]
- Massol RH, Boll W, Griffin AM, Kirchhausen T. A burst of auxilin recruitment determines the onset of clathrin-coated vesicle uncoating. *Proc Natl Acad Sci U S A*. 2006; 103:10265–10270. [PubMed: 16798879]
- Perera RM, Zoncu R, Lucast L, De Camilli P, Toomre D. Two synaptojanin 1 isoforms are recruited to clathrin-coated pits at different stages. *Proc Natl Acad Sci U S A*. 2006; 103:19332–19337. [PubMed: 17158794]
- Peter BJ, Kent HM, Mills IG, Vallis Y, Butler PJ, Evans PR, McMahon HT. BAR domains as sensors of membrane curvature: the amphiphysin BAR structure. *Science*. 2004; 303:495–499. [PubMed: 14645856]
- Raimondi A, Ferguson SM, Lou X, Armbruster M, Paradise S, Giovedi S, Messa M, Kono N, Takasaki J, Cappello V, et al. Overlapping role of dynamin isoforms in synaptic vesicle endocytosis. *Neuron*. 2011; 70:1100–1114. [PubMed: 21689597]
- Ralser M, Nonhoff U, Albrecht M, Lengauer T, Wanker EE, Lehrach H, Krobitsch S. Ataxin-2 and huntingtin interact with endophilin-A complexes to function in plastin-associated pathways. *Hum Mol Genet*. 2005; 14:2893–2909. [PubMed: 16115810]
- Ringstad N, Gad H, Low P, Di Paolo G, Brodin L, Shupliakov O, De Camilli P. Endophilin/SH3p4 is required for the transition from early to late stages in clathrin-mediated synaptic vesicle endocytosis. *Neuron*. 1999; 24:143–154. [PubMed: 10677033]
- Ringstad N, Nemoto Y, De Camilli P. The SH3p4/Sh3p8/SH3p13 protein family: binding partners for synaptojanin and dynamin via a Grb2-like Src homology 3 domain. *Proc Natl Acad Sci U S A*. 1997; 94:8569–8574. [PubMed: 9238017]
- Ringstad N, Nemoto Y, De Camilli P. Differential expression of endophilin 1 and 2 dimers at central nervous system synapses. *J Biol Chem*. 2001; 276:40424–40430. [PubMed: 11518713]

- Sankaranarayanan S, Ryan TA. Real-time measurements of vesicle-SNARE recycling in synapses of the central nervous system. *Nat Cell Biol.* 2000; 2:197–204. [PubMed: 10783237]
- Schuske KR, Richmond JE, Matthies DS, Davis WS, Runz S, Rube DA, van der Bliet AM, Jorgensen EM. Endophilin is required for synaptic vesicle endocytosis by localizing synaptojanin. *Neuron.* 2003; 40:749–762. [PubMed: 14622579]
- Sundborger A, Soderblom C, Vorontsova O, Evergren E, Hinshaw JE, Shupliakov O. An endophilin-dynamin complex promotes budding of clathrin-coated vesicles during synaptic vesicle recycling. *J Cell Sci.* 2011; 124:133–143. [PubMed: 21172823]
- Traub LM. Tickets to ride: selecting cargo for clathrin-regulated internalization. *Nat Rev Mol Cell Biol.* 2009; 10:583–596. [PubMed: 19696796]
- Trempe JF, Chen CX, Grenier K, Camacho EM, Kozlov G, McPherson PS, Gehring K, Fon EA. SH3 domains from a subset of BAR proteins define a Ubl-binding domain and implicate parkin in synaptic ubiquitination. *Mol Cell.* 2009; 36:1034–1047. [PubMed: 20064468]
- Verstreken P, Kjaerulff O, Lloyd TE, Atkinson R, Zhou Y, Meinertzhagen IA, Bellen HJ. Endophilin mutations block clathrin-mediated endocytosis but not neurotransmitter release. *Cell.* 2002; 109:101–112. [PubMed: 11955450]
- Verstreken P, Koh TW, Schulze KL, Zhai RG, Hiesinger PR, Zhou Y, Mehta SQ, Cao Y, Roos J, Bellen HJ. Synaptojanin is recruited by endophilin to promote synaptic vesicle uncoating. *Neuron.* 2003; 40:733–748. [PubMed: 14622578]
- Voglmaier SM, Kam K, Yang H, Fortin DL, Hua Z, Nicoll RA, Edwards RH. Distinct endocytic pathways control the rate and extent of synaptic vesicle protein recycling. *Neuron.* 2006; 51:71–84. [PubMed: 16815333]
- Weston MC, Nehring RB, Wojcik SM, Rosenmund C. Interplay between VGLUT isoforms and endophilin A1 regulates neurotransmitter release and short-term plasticity. *Neuron.* 2011; 69:1147–1159. [PubMed: 21435559]
- Yim YI, Sun T, Wu LG, Raimondi A, De Camilli P, Eisenberg E, Greene LE. Endocytosis and clathrin-uncoating defects at synapses of auxilin knockout mice. *Proc Natl Acad Sci U S A.* 2010; 107:4412–4417. [PubMed: 20160091]

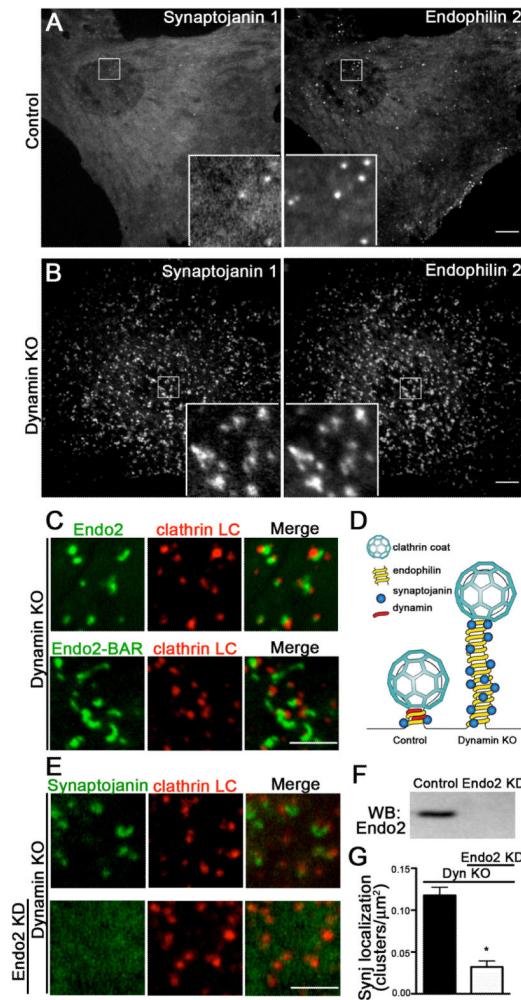


Figure 1. The recruitment of synaptojanin 1-145 at endocytic pits is dynamin independent, but requires endophilin

Control fibroblasts and fibroblasts that lack expression of dynamin 1 and 2 (dynamin KO) were transfected with fluorescent proteins and examined by spinning disk confocal microscopy.

(A) and (B) Endophilin 2-Ruby and EGFP-synaptojanin 1 precisely colocalize in both control and dynamin KO cells (magnified in the inset). The few fluorescent spots in control cells represent very late pits (Perera et al., 2006) while the numerous puncta in dynamin KO cells represent arrested CCPs. Bar=10µm.

(C) Both C-terminally EGFP-tagged full length (FL) endophilin 2 and endophilin 2 BAR domain (1–247) are recruited to the arrested CCPs in dynamin KO cells also expressing mRFP-clathrin LC. Bar=5µm

(D) Model of endophilin and synaptojanin localization at the necks of the CCPs in cells with and without dynamin.

(E–G) Dynamin DKO cells were transfected with synaptojanin 1-145-EGFP and clathrin LC-mRFP after siRNA-dependent KD of endophilin 2 (the major isoform in fibroblasts). (E) The synaptojanin 1–145 puncta visible in control siRNA treated cells (reflecting protein on the tubular necks of the pits) are drastically reduced after endophilin 2 KD, whose effectiveness is demonstrated by the western blot of (F). 96.0%±1.5% of the synaptojanin spots were directly adjacent to clathrin puncta (n=194 synaptojanin spots from 5 cells). Bar=5µm.

(G) Quantification of the synaptojanin puncta density in the two conditions (8 cells/condition, $p=0.0002$).

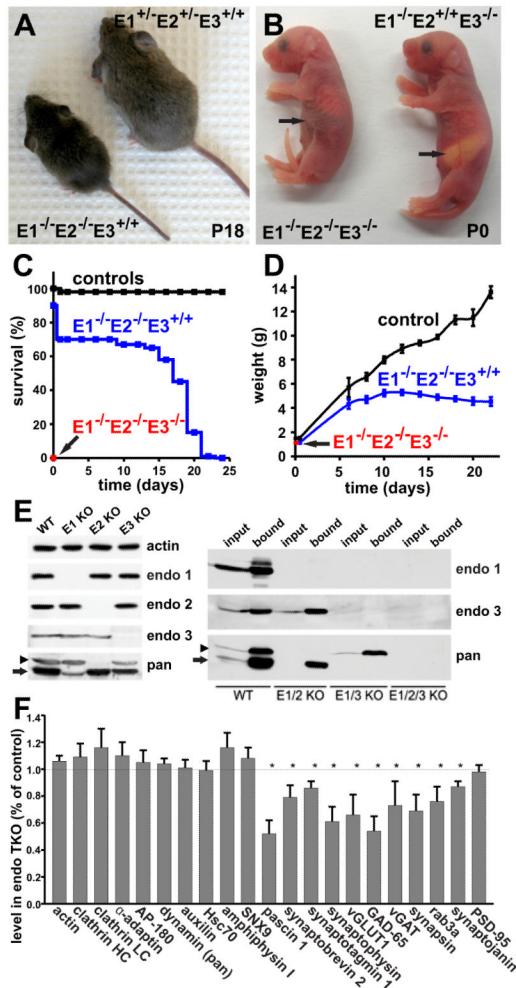


Figure 2. Absence of endophilin causes perinatal lethality

(A) Endophilin 1,2 double KO (DKO) mouse and control littermate heterozygous for endophilin 1 and 2 at P18. Note the smaller size of the DKO mouse.

(B) Endophilin triple KO (TKO) newborn mouse and control littermate WT for endophilin 2. Note absence of milk (arrows) in the stomach of the TKO.

(C) Survival curves of endophilin TKOs, endophilin 1,2 DKO mice and control mice derived from the same litters.

(D) Weight at birth and growth curves of endophilin mutant mice. Note the early arrest of growth of endophilin 1,2 DKO mice, but the steady growth of control littermates. Mean \pm SEM of mice from at least 14 litters.

(E) Immunoblot analysis of brain homogenates (left) and GST pull-downs (right) from WT and endophilin KO mice with anti-endophilin isoform-specific antibodies and anti-pan-endophilin antibody. Endophilin 1 and 3 have the same electrophoretic motility (arrow), while endophilin 2 has a slower motility (arrowhead). The relevant endophilins are absent in the corresponding KO material. Note (left panel) that the absence of endophilin 1 has a greater impact than the absence of endophilin 3 on the intensity of the pan-endophilin band (arrow), indicating the greater abundance of endophilin 1 in brain. There is no difference in the expression of the remaining endophilins in the corresponding KOs. Right panel: blots of GST pull-downs from WT, DKO and TKO brain extracts using synaptojanin 1's PRD domain as a bait.

(F) Histogram showing levels of synaptic proteins, as detected by quantitative immunoblotting, in brain extracts of TKO newborn mice normalized to WT. The TKO extracts show reduced levels of many SV proteins. Bars=mean±SEM (N≥4, *p<0.05, t-test).

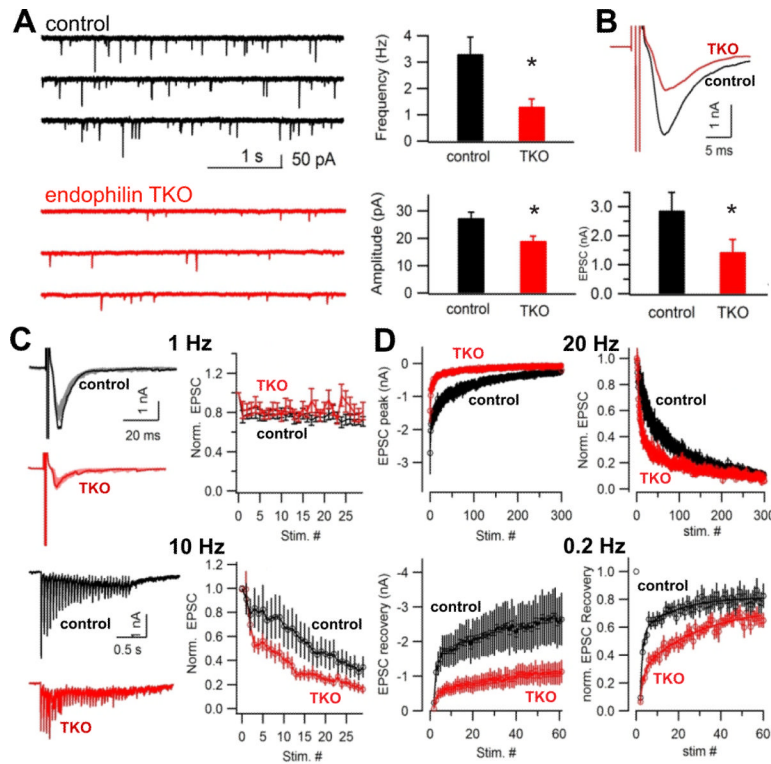


Figure 3. Synaptic transmission is impaired but not abolished in endophilin TKO neurons

(A) Reduced frequency of spontaneous mEPSCs in TKO neurons (* $p=0.007$, t-test). The amplitude is also slightly reduced (* $p=0.007$, t-test).

(B) The amplitudes of EPSCs in response to a single action potential (AP) are smaller in the TKO ($N=20$) than in control ($N=19$) neurons (* $p=0.0027$, two-tail wilcoxon test).

(C) Synaptic depression in response to 30 APs delivered at low (1 Hz) and high (10 Hz) frequency. Left panels show examples of individual recordings (in the 1 Hz recordings, AP traces are superimposed). Right panels, which show control ($N=19$) and TKO ($N=20$) responses normalized to the first EPSC, demonstrate a difference only at the 20 Hz stimulation.

(D) Decline of EPSC peak amplitude in response to a longer stimulation (300 AP delivered at 20 Hz; upper panels) and subsequent recovery upon interruption of the stimulus as detected by a 0.2 Hz test stimuli (lower panels). Depression occurred faster and recovered slower in TKO ($N=17$) relative to WT ($N=17$) neurons. EPSCs were normalized to the EPSC peak amplitude of the train.

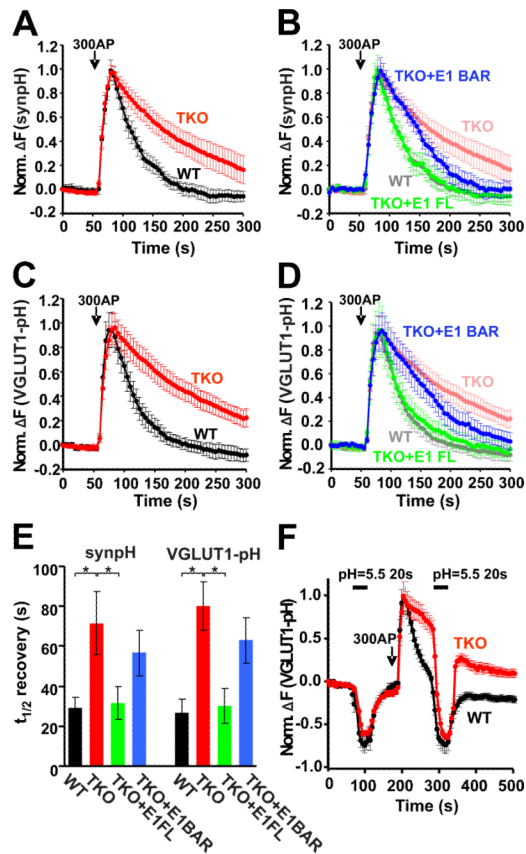


Figure 4. Compensatory endocytic recovery is slower in endophilin TKO neurons

(A–B) The average time-course of the endocytic recovery after a 10 Hz 300 AP stimulus, as measured by synaptopHluorin (N=14 for WT, 13 for TKO) and vGLUT1-pHluorin (N=16 for both WT and TKO) is slower in TKO than in WT. Arrows mark the start of the stimuli. Values shown are mean \pm SEM.

(C–D) Overexpression of full length endophilin 1-mRFP rescues the slower endocytic recovery of synaptopHluorin and vGLUT1-pHluorin signals, respectively (green traces). In contrast, an endophilin BAR construct (aa1-290)-mRFP shows only a partial rescue of the endocytic defect, which is more prominent during the late phase of the recovery (blue traces). The green and blue traces from the rescue experiments are superimposed on the recoveries shown in (A) and (B) to allow a direct comparison of the kinetics of recovery. (E) Average $t_{1/2}$ recovery times for the conditions shown in (A–D). * $p < 0.05$, t-test, error bars=SEM.

(F) The delayed recovery from the increase of pHluorin fluorescence is not due to a defect in reacidification of newly endocytosed vesicles. Neurons expressing vGLUT1-pHluorin were briefly exposed to pulses of extracellular acid solution (pH 5.5) at the times indicated. In both WT (N=8) and TKO (N=8), the fluorescence quenched consistently to the same levels before and after the stimulus, arguing against a lag in the acidification of a newly internalized vesicle pool.

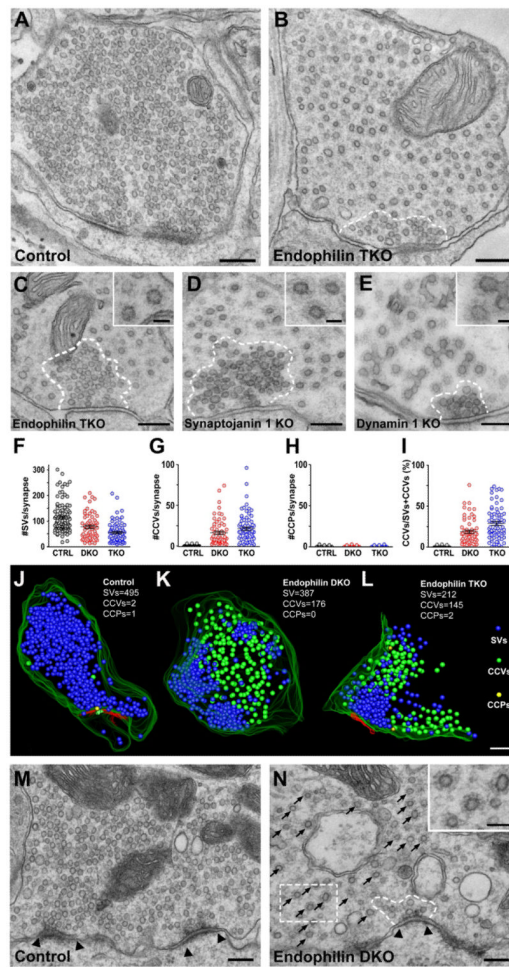


Figure 5. Increased number of clathrin-coated vesicles, but not clathrin-coated pits at endophilin DKO and TKO synapses

(A–B) EM ultrastructure of control (WT) and endophilin TKO synapses from cortical neuronal cultures (DIV21). SVs occupy nearly the entire control nerve terminal, while in the TKO synapse, the few SVs (outlined by dashed white line) are surrounded by numerous CCVs, which are sparsely packed and embedded in a dense cytomatrix. Bars=200 nm.

(C–E) Endophilin TKO, synaptojanin 1 KO and dynamin 1 KO synapses, respectively. In all three synapses, a cluster of densely packed SVs (white dashed line) is surrounded by abundant coated vesicular profiles, but only in dynamin 1 KO synapses examples of such structures with elongated necks in the plane of the section can be seen. Bars=250 nm. Insets: higher magnification of clathrin-coated structures. Bars=50 nm.

(F–I) Morphometric analysis of SVs, CCVs and CCPs in control and endophilin mutant synapses. The ratio of CCVs to total (CCVs+SVs) vesicles is shown in I. Each circle represents one synapse.

(J–L) 3D models of control, endophilin DKO and TKO synapses derived from the reconstruction of 300 nm-thick tomograms showing SVs (blue), CCVs (green) and CCPs (yellow). Green and red lines show plasma membrane and the postsynaptic density, respectively. Bars=200 nm.

(M–N) Synapses from the same brain stem region in control and DKO mice at P9. Note the only few SVs anchored to the active zone (arrowheads) and the numerous CCVs (arrows and inset) in the DKO synapse. Bars=200 nm, inset=100 nm.

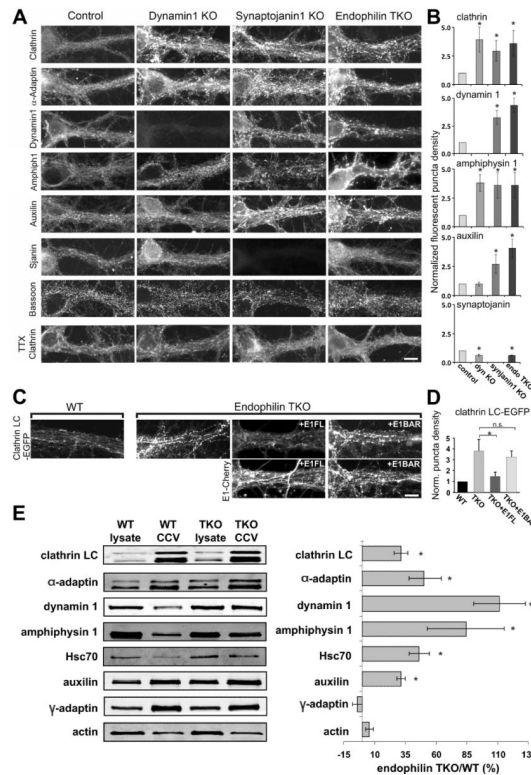


Figure 6. Redistribution of endocytic proteins at endophilin TKO synapses

(A) Immunofluorescence of the proteins indicated at left in cortical neuronal cultures (DIV 18–24) from control, dynamin 1 KO, synaptojanin 1 KO and endophilin TKO mice.

Clathrin, α -adaptin and amphiphysin 1 are predominantly diffuse in control neurons, but clustered in all three mutant genotypes. Dynamin 1 and auxilin are clustered in synaptojanin and endophilin mutant synapses, but auxilin is not clustered in dynamin 1 KO. Synaptojanin is slightly more diffuse in the absence of endophilin. The punctate Bassoon immunofluorescence is similar in all genotypes. Following treatment with TTX (1 μ M, 14–18 h) to silence neuronal activity, clathrin was no longer clustered. Bar=15 μ m.

(B) Quantification of the clustering of immunoreactivity. The y-axis represents the fold increase of fluorescence puncta in mutant synapses normalized to controls. * p <0.05, t-test. Bars=mean \pm SEM.

(C) Fluorescence analysis of EGFP-clathrin LC in WT and endophilin TKO neurons (DIV 18–24). Clathrin is predominantly diffuse in control neurons, but clustered in endophilin TKOs. Clustering was rescued by expression of endophilin 1 FL-Cherry, but not of the endophilin 1 BAR-Cherry construct.

(D) Quantification of the clustering of the clathrin fluorescence in the four conditions shown in (C). The y-axis represents the fold increase of fluorescence puncta in mutant synapses normalized to WT. Bars=mean \pm SEM, n.s. not significant, * p <.05, t-test.

(E) Left: Western blot analysis of starting lysates and CCV enriched fractions obtained from WT and endophilin TKO primary cultures (DIV 21). Right: Levels of proteins in the CCV enriched fractions from endophilin TKO cultures normalized to the WT values. Bars=mean \pm SEM, * p <0.05, t-test.

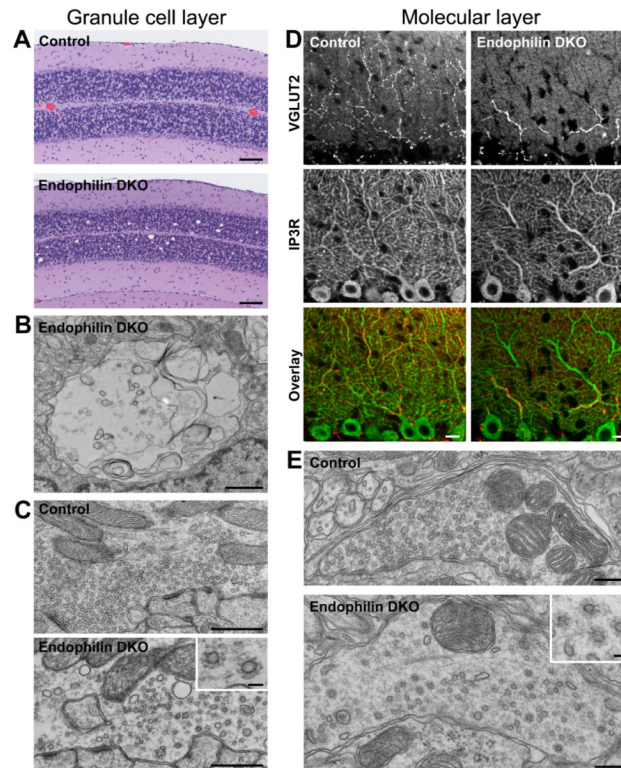


Figure 7. Neurodegeneration in endophilin 1, 2 DKO mice (P18)

(A) H&E stained cerebellar cortex of control (E1^{+/-}E2^{+/-}E3^{+/+}) and endophilin DKO mice. Unstained vacuolar structures, suggesting a form of spongiform neurodegeneration, are present in DKO granule cell layer. Bars=100 μ m.

(B) EM of the DKO granule cell layer showing a vacuolar structure filled with membranous debris. Bars=1 μ m.

(C) EM of mossy fiber synapses in control and DKO cerebella. Note in the DKO the low number of SVs and the presence of sparsely packed CCVs (higher magnification in the inset). Bars=500 nm, inset 50 nm.

(D) Morphology of climbing fibers (top row), as revealed by immunofluorescence for vGLUT2, in control and DKO mice. Sections were counterstained for the IP₃ receptor, a Purkinje cell marker (middle row). Note in the overlay image that climbing fibers in the DKOs are swollen and do not extend beyond the most proximal portion of Purkinje cell dendrites. Bars=20 μ m.

(E) EM of climbing fiber synapses. Note the low number of SVs and the presence of sparsely packed CCVs (higher magnification in the inset) in the DKOs. Bars=250 nm, inset 50 nm.

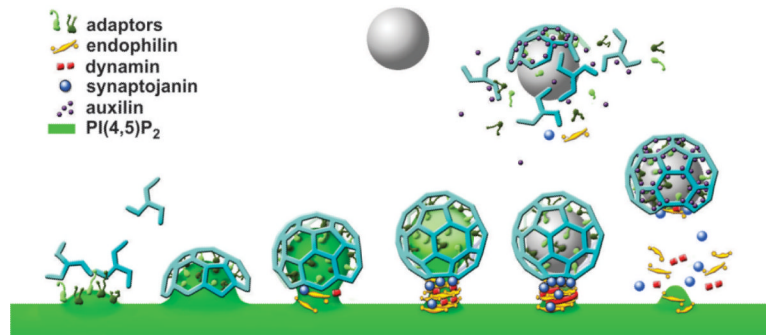


Figure 8. Putative model of clathrin-coated vesicle fission and uncoating at synapses

Assembly and early maturation of endocytic CCPs is independent of endophilin. Endophilin is recruited only to the neck of late stage pits. The dynamin-endophilin interaction may regulate dynamin function, but it is dispensable for dynamin recruitment and for fission. In contrast, the synaptojanin-endophilin interaction is critically important for the fate of the vesicle after fission. Loss of PI(4,5)P₂ on the bud may start before fission and be restricted to the bud due to the presence of a collar comprising endophilin, other BAR proteins and dynamin (see Discussion). Auxilin recruitment and uncoating are triggered only after fission.